

The effect of variations in irradiance on buoyancy regulation in *Microcystis aeruginosa*

Brett B. Wallace and David P. Hamilton

Department of Environmental Engineering, Centre for Water Research, University of Western Australia, Nedlands, WA 6907, Australia

Abstract

A mechanism of buoyancy regulation in cyanobacteria was investigated in a fluctuating light environment typical of the mixed layer in a lake. New measurements of density and cellular carbohydrate content were obtained from a field sample of the cyanobacterium *Microcystis aeruginosa*. The rate of increase in carbohydrate and density in this cyanobacterium does not instantaneously adjust to an increase in light intensity. There is a time lag, the response time, corresponding to physiological adjustment to the increase in light, before equilibration of the rate of carbohydrate and density increase. Also, the rate of density and carbohydrate increase is nonlinear over the response time. Based on these experimental findings, a new model for buoyancy regulation was developed that includes the response time. This model was applied to two fluctuating light regimes that simulate Langmuir circulation and turbulence. The simulations reveal that the response time is critical in determining if a cell equilibrates its rate of density change to a change in the light that it receives. If the response time is longer than the time scale of the light fluctuation, then the rate of density increase will be less than the optimal equilibrium rate. Models that do not include the response time will not correctly predict the buoyancy of cyanobacteria and their water column position after an episode of mixing.

The existence of cyanobacteria that can regulate their buoyancy has been well documented (Walsby 1969a, 1970; Oliver and Walsby 1984; Utkilen et al. 1985; Thomas and Walsby 1986; Kromkamp et al. 1986; Humphries and Lyne 1988; Zohary and Robarts 1989; Kromkamp and Walsby 1990; Ibelings et al. 1991; Walsby et al. 1991). This characteristic is considered to be important in contributing to the success of cyanobacteria in a wide range of aquatic ecosystems (Reynolds and Walsby 1975; Reynolds 1984, 1987; Reynolds et al. 1987) because it provides the advantage of being able to alter position in the water column through physiological changes. Ganf and Oliver (1982) showed how buoyancy regulation allowed cyanobacteria to overcome the vertical separation of light and nutrients in a stratified lake.

There are three mechanisms of buoyancy regulation. The first is changes in cell ballast (Oliver and Walsby 1984; Thomas and Walsby 1986; Kromkamp et al. 1988) resulting from the accumulation or consumption of storage molecules. The second mechanism is regulation of gas vesicle synthesis (Walsby 1969b), which depends on light (Deacon and Walsby 1990) and macronutrients such as nitrogen and carbon (Klemer 1978, 1991). If gas vesicle synthesis ceases, buoyancy may be lost as the cellular concentration of gas vesicles is diluted by cell growth and division (Walsby et al. 1983). The third mechanism is irreversible collapse of gas vesicles under rising turgor pressure (Walsby 1971) generated through the photosynthetic production of low-molecular-weight carbohydrates (Grant and Walsby 1977) and by light-dependent uptake of potassium ions (Allison and Walsby 1981). However, this mechanism probably is not responsible for buoyancy regulation in most natural populations (Walsby

1994). Also, many species such as *Microcystis aeruginosa* have gas vesicles too strong to be collapsed by turgor or hydrostatic pressures (Utkilen et al. 1985; Kromkamp et al. 1986; Thomas and Walsby 1986). Even in organisms with collapsible gas vesicles, the initial changes in buoyancy are caused by changes in ballast (Kromkamp et al. 1986). Cell ballast is the short-term mechanism of buoyancy regulation in most, if not all, gas vacuolate cyanobacteria (Oliver et al. 1985; Thomas and Walsby 1986; Kromkamp and Walsby 1990).

Cell ballast is usually increased by the storage of carbohydrate (Thomas and Walsby 1986), although under phosphorus-enriched conditions the storage of polyphosphate and possibly other molecules contributes to cell ballast (Konopka et al. 1993). Kromkamp and Walsby (1990), Howard et al. (1996), and Visser et al. (1997) investigated rates of carbohydrate accumulation in attempts to mathematically quantify the effects of ballast changes on buoyancy. In these studies, carbohydrate ballast accumulation was assumed to be a linear function of time. However, our experimental results show that carbohydrate ballast accumulation is nonlinear over a period of adjustment in response to an increase in light intensity. As a consequence, cell density also changes nonlinearly during this period of adjustment.

A mathematical model of the nonlinear adjustment period was developed. The model is based on equations similar to those used by Pahl-Wostl and Imboden (1990) to describe the adjustment of photosynthetic rates in response to changes in irradiance. This new model was used to investigate the effect of the nonlinear response on the buoyancy regulation of cyanobacteria exposed to two different types of light fluctuations that may be commonly experienced during mixing events in natural aquatic environments. The first type is organized periodic light fluctuations similar to what would be experienced by cells entrained in Langmuir circulation cells (Langmuir 1938). The second type is disorganized random light fluctuations such as what would be experienced in tur-

Acknowledgments

We thank A. Hobbs and C. Ranasinghe for advice on using the Percoll density marker beads and for help producing the Percoll gradients. We also thank Anya Waite, Rod Oliver, and the two anonymous reviewers for their critical reviews of the manuscript.

bulence. The results show that the relationship between the adjustment time and the intensity and duration of light fluctuations experienced in a mixing event determines the buoyancy of the cyanobacteria. The adjustment time also determines, under certain conditions, whether the cyanobacteria will sink or float once a mixing event subsides.

Methods

Apparatus—A sample of gas vacuolate *Microcystis aeruginosa* Kütz. emend. Elenkin. was taken from Lake Yangebup in Western Australia during a bloom in June 1997. The field sample was transferred directly to the laboratory and placed in three baffled 600-ml flasks. Prior to the commencement of the experiment, the samples were kept in the dark for 15 min to equilibrate to the laboratory conditions. The sample was bubbled with air (70 liters h^{-1}) to ensure CO_2 saturation and also to mix the sample to ensure the colonies were evenly distributed during the experiment. The experiment was conducted with all samples at a constant temperature of 20°C .

A 500-W tungsten spotlight (General Electric) was used as the light source for the experiments. The light was filtered through a water bath constructed from 1-cm-thick perspex sheets enclosing a 4-cm-thick layer of water and a 1-cm-thick layer of copper sulfate solution (20 g liter^{-1}) to remove virtually all wavelengths of light $>720 \text{ nm}$ (Marra 1978). The maximum light intensity available was $1,300 \mu\text{mol photons m}^{-2} \text{ s}^{-1}$, a typical midday surface light intensity. Screens made of tissue paper were used to filter the light down to intensities of $300 \mu\text{mol}$ and $50 \mu\text{mol photons m}^{-2} \text{ s}^{-1}$.

Measurements—Cells were pressurized (1.5 MPa) to collapse the gas vesicles, and their density was measured using Percoll density gradients (Oliver et al. 1981). The Percoll gradients were osmotically adjusted to the density of the lake water (Kromkamp and Mur 1984). The Percoll gradients were performed by centrifuging at $40,000 \times g$ for 20 min at 20°C in a Beckman J2-MC centrifuge with an angle head rotor. A 1-ml sample of *Microcystis* was layered on top of the Percoll gradient and spun in a benchtop centrifuge with an angle head rotor for 4 min at $800\text{--}2,000 \times g$. The density of the cells was determined by visually reading the position of the band of cells relative to the position of the precalibrated density marker beads (Parnacia) that were placed in each gradient (Kromkamp and Mur 1984). Carbohydrate was determined with the anthrone reagent and D-glucose standards (Hebbert et al. 1971). Carbohydrate measurements were taken in duplicate.

Results

Experiments—The simplest experiment to use to investigate the effect of fluctuating light on the change in density of the *Microcystis* cells is to consider only one fluctuation. We used the extreme case of an instantaneous increase from zero to constant irradiance and took measurements of carbohydrate at 10-min intervals for the first hour, followed by hourly measurements for the subsequent 5 h. Density mea-

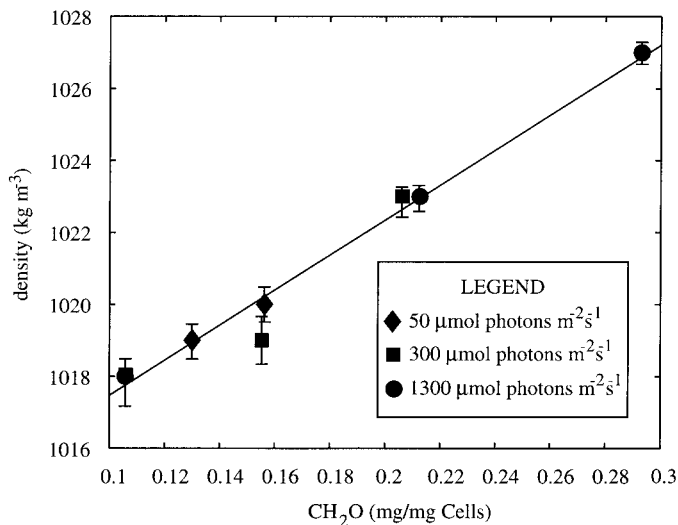


Fig. 1. Cell density plotted against carbohydrate content of the cells of *Microcystis aeruginosa*. The data are fitted with a linear fit (solid line) with $R^2 = 0.9887$. The error bars on the density measurements represent the range of densities encompassed by the band of cells measured in the Percoll gradient.

surements of the *Microcystis* were taken at the start of the experiment, after 3 h, and after 6 h for each of the three irradiances. These measurements are plotted against the corresponding carbohydrate measurements in Fig. 1.

There is a strong linear relationship between cell density without gas vesicles and cellular carbohydrate (Fig. 1). Using linear regression analysis a line (with $R^2 = 0.9887$) is fitted to the data. The line is given by the equation

$$\rho = mC + b, \quad (1)$$

where ρ is the cell density (kg m^{-3}), C is the carbohydrate content (mg/mg cells), $m = 48.7 \text{ kg m}^{-3} (\text{mg/mg Cells})^{-1}$, and $b = 1012.6 \text{ kg m}^{-3}$. Equation 1 was used to calculate density values corresponding to the carbohydrate measurements made during the experiment.

The results of the experiment are shown in Fig. 2. The rate of change of density with time was not constant; instead, it increased from zero to a constant value over a time period of approximately 20 min. Once a constant rate of change of density was reached, the density increased at this rate until the maximum density was attained, in agreement with the findings of Kromkamp and Walsby (1990). The magnified view of the first hour of the experiment (Fig. 2C) shows that there was a nonlinear rate of change of density with time. This nonlinearity was more pronounced for the light exposure of $1,300 \mu\text{mol photons m}^{-2} \text{ s}^{-1}$ than for the 300 or $50 \mu\text{mol photons m}^{-2} \text{ s}^{-1}$ data.

Figure 2E shows the relationship between density change and light intensity for different light exposure times. For each of the three irradiances, the difference is plotted between the measured density after 10 min, 20 min, and 1 h and the measured density at 0 min, 10 min, and 50 min, respectively. These points do not define a single curve but rather a family of curves that depend on time.

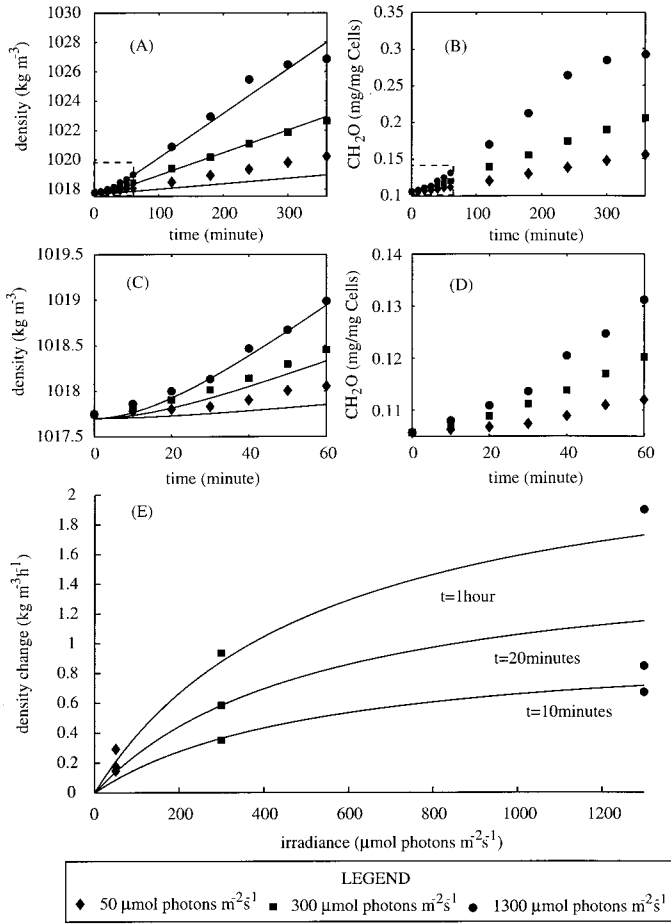


Fig. 2. Comparison of the model Eq. 7 (solid line) and experimental results. (A) Density versus time, where density is determined from Eq. 1 and the carbohydrate measurements are shown in (B). (C) and (D) are enlarged views of the areas enclosed in the dashed boxes in (A) and (B), respectively. (E) The rate of density change versus irradiance. The experimental data points are the rate of density change over 0–10 min, 10–20 min, and 50–60 min. The model results are the rate of density change at 10 min, 20 min, and 60 min.

Model description—We propose a mathematical description of buoyancy regulation that describes the temporal dependence of the rate of change of density (D) to changing light intensity (I). As a consequence, D does not simply depend on the actual light I , as is the case in all existing models; it also depends on the prior light history, as follows:

$$\frac{dD}{dt} = K_r(D - D_{eq}) \quad (2)$$

where D_{eq} is the equilibrium value of D and K_r is given by:

$$K_r = \begin{cases} \frac{1}{\tau_r}; & \text{for increasing light} \\ 0; & \text{for decreasing light} \end{cases} \quad (3)$$

where τ_r is the response time.

A model for D_{eq} has been proposed by Kromkamp and Walsby (1990):

$$D_{eq}(I) = \frac{d\rho(I)}{dt} = c_1 \frac{I(t)}{K_I + I(t)} - c_3 \quad (4)$$

where ρ is the cell density, c_1 is defined as the rate constant determining the increase in density with time, K_I is the irradiance at which the rate of density increase with time is half the maximal rate, and c_3 is the minimum rate of density decrease in the dark.

Howard et al. (1996) and Visser et al. (1997) suggested different mathematical descriptions for D_{eq} . Howard et al. (1996) related photosynthetic rate to the rate of carbohydrate accumulation through parametric equations, and Visser et al. (1997) included inhibition effects at high irradiances. However, both of these mathematical descriptions assume that the rate of density change in response to light is linear with time, as in Kromkamp and Walsby's (1990) description. Other differences between the models are not relevant for what follows and the Kromkamp and Walsby form of D_{eq} is retained.

Equation 2 can be solved using an appropriate transform method (e.g., Laplace transform) to give the solution

$$D(t) = e^{-(t/\tau_r)}D(0) + \frac{1}{\tau_r} \int_0^t D_{eq}(t')e^{-(t-t')/\tau_r} dt' \quad (5)$$

where $D(0)$ is the previous value of D . Thus, our model introduces a transient response term τ_r and a dependence on the previous rate of density change $D(0)$. This model was calibrated against our measured data assuming a light regime of the form

$$I = \begin{cases} I_0, & t \geq 0 \\ 0, & t < 0 \end{cases} \quad (6)$$

where I_0 is the value of the constant irradiance. Substituting this into Eq. 5 gives

$$D(t) = \left(c_1 \frac{I_0}{K_I + I_0} - c_3 \right) (1 - e^{-(t/\tau_r)}) \quad (7)$$

where $D(0) = 0$. The values of the model parameters after calibration with our data are $c_1 = 0.0427 \text{ kg m}^{-3} \text{ min}^{-1}$, $K_I = 530 \text{ } \mu\text{mol photons m}^{-2} \text{ s}^{-1}$, $c_3 = 4.6 \times 10^{-6} \text{ kg m}^{-3} \text{ min}^{-1}$, and $\tau_r = 20 \text{ min}$. Using these parameter values, Eq. 7 is plotted against our measured data in Fig. 2. The model accurately predicts the change in density (ρ) with time shown in Fig. 2A and Fig. 2C for intensities of $300 \text{ } \mu\text{mol photons m}^{-2} \text{ s}^{-1}$ and $1,300 \text{ } \mu\text{mol photons m}^{-2} \text{ s}^{-1}$. Comparison of model predictions against the measured rate of density change, D , is shown in Fig. 2E. Our model results agree with the measured values and illustrate that the relationship between density change and irradiance depends on time. As time becomes large compared with the response time, the relationship between density change and irradiance reaches equilibrium ($D \rightarrow D_{eq}$ as $e^{-t/\tau_r} \rightarrow 0$, see Eq. 7).

The data at the $50 \text{ } \mu\text{mol photons m}^{-2} \text{ s}^{-1}$ light intensity is, however, slightly underpredicted by our model. This error could be explained by variability about the regression line given by Eq. 4 and is a reflection of the uncertainties in the measured data rather than problems with the model itself. There is also a reduction in the measured rate of carbohydrate accumulation after 5 h of exposure at the $1,300 \text{ } \mu\text{mol}$

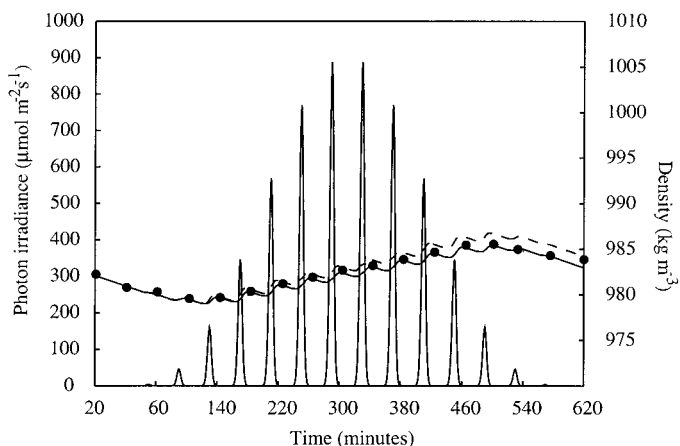


Fig. 3. Changes in cell density in response to a fluctuating irradiance regime. The measured data (dots) are from Visser et al. (1997) and are plotted against the predicted values of Visser et al. (dashed line) and our model (solid line) for a response time of $\tau_r = 4$ min.

photons $\text{m}^{-2} \text{s}^{-1}$ intensity as the cells reach their maximum storage capacity of carbohydrate (see Fig. 2B).

Model validation—The model was validated with measurements (Visser et al. 1997) of carbohydrate content in continuous cultures of *Microcystis* exposed to a fluctuating light regime (Fig. 3). Visser et al. (1997) suggested a mathematical description of D_{eq} , based on their measured data, that incorporates inhibition of density change at high irradiances:

$$D_{eq} = \frac{No}{60} I e^{-I/I_0} + e \quad (8)$$

where I_0 is the inhibition intensity of density increase, No is a correction factor, and e is the rate of density change at $I = 0$. From Visser et al. (1997), $I_0 = 277.5 \mu\text{mol photons m}^{-2} \text{s}^{-1}$, $No = 0.0945 \text{ kg m}^{-3} \mu\text{mol photons}^{-1} \text{ m}^2$, and $e = -0.0165 \text{ kg m}^{-3} \text{ min}^{-1}$.

To validate our model, we substituted Eq. 8 into Eq. 5 and plotted the results against the measurements of Visser et al. (1997) and the values predicted by Eq. 8. Figure 3 shows that Eq. 8 slightly overpredicts the measured values during the second part of the photoperiod, as noted by Visser et al. (1997). However, the results from Eq. 5 are almost identical to the measured values for a response time $\tau_r = 4$ min.

Model application

The model was applied to three cases: (1) a water body with no water motion, (2) a simple model of Langmuir circulation representing organized water motion, and (3) a simple model of turbulence representing random water motion. In all of these scenarios the surface light intensity is assumed to be of the form

$$I_0 = I_{\max} \sin^3\left(\frac{\pi t}{T}\right) \quad (9)$$

where T is the photoperiod (12 h) and I_{\max} is the surface light intensity set to $1,500 \mu\text{mol photons m}^{-2} \text{s}^{-1}$. Light intensity decreases with water depth according to Beer's Law:

$$I(z) = I_0 e^{-\eta z} \quad (10)$$

where $I(z)$ is the irradiance at depth z and η is the attenuation coefficient (set to $\eta = 1.5 \text{ m}^{-1}$ for all simulations presented).

The model equation governing buoyancy regulation in the dark, when $I(z) \leq 0.05 I_{\max}$, is taken from Kromkamp and Walsby (1990). Density change in the dark could be described as a linear function of the previous irradiance (I_a):

$$D = \frac{d\rho}{dt} = -c_2 I_a - c_3 \quad (11)$$

where c_2 is a parameter describing the rate of density decrease above the minimal rate, c_3 , and I_a is the average irradiance history. In our model, we set $c_2 = 1.67 \times 10^{-5} \text{ kg m}^{-3} \text{ min}^{-1} (\mu\text{mol photons m}^{-2} \text{s}^{-1})^{-1}$ and I_a as the integrated value of irradiance accumulated since dawn (see Kromkamp and Walsby 1990).

Buoyant cells (with gas vesicles) are simulated, although our measured densities are of cells with collapsed gas vesicles. Therefore, the nonbuoyant cell densities are converted to buoyant cell densities by subtracting the difference between the initial nonbuoyant cell density of 1017.7 kg m^{-3} that was measured in the experiment and the buoyant cell density of 990 kg m^{-3} that was used as the starting density for all simulations (see Visser et al. 1997).

The sinking or rising velocity v of a colony can be determined using Stokes's equation

$$v = \frac{2gr^2(\rho - \rho_w)}{9\phi\mu} \quad (12)$$

where g is gravitational acceleration, r is the effective colony radius, ϕ is the form resistance of the colony (which for *Microcystis* was set to 1 after Reynolds et al. 1987), μ is the viscosity of the water (assumed to be constant at $1 \times 10^{-3} \text{ kg m}^{-1} \text{s}^{-1}$), and ρ_w is the ambient density of the water (assumed here to be constant at 998 kg m^{-3}).

Case 1—The results of simulations for case 1 are presented in Fig. 4. The depth trajectories in response to the light regime shown in Fig. 4A are plotted in Fig. 4B for single colonies. Initially, the colonies were buoyant (Fig. 4C) and floated on the surface until just after midday, when they had accumulated enough ballast to lose their buoyancy. The depth trajectories for two colony sizes ($200 \mu\text{m}$ and $800 \mu\text{m}$) are shown, with the larger colony size sinking to greater depth than the smaller one. The time taken for the colonies to become heavier than the ambient water and to begin to sink is dependent on the response time. The colony with no response time ($D = D_{eq}$) is first to lose buoyancy. As a result, the $800\text{-}\mu\text{m}$ colony with the 20-min response time will reach a lower density and make a shallower migration than the $800\text{-}\mu\text{m}$ colony with no response time. Additionally, the $800\text{-}\mu\text{m}$ colony with the longer response time receives a higher light dose and regains buoyancy slightly faster than do the other $800\text{-}\mu\text{m}$ colonies. In all other respects, the model behaves identically to all previous models that predict D_{eq} .

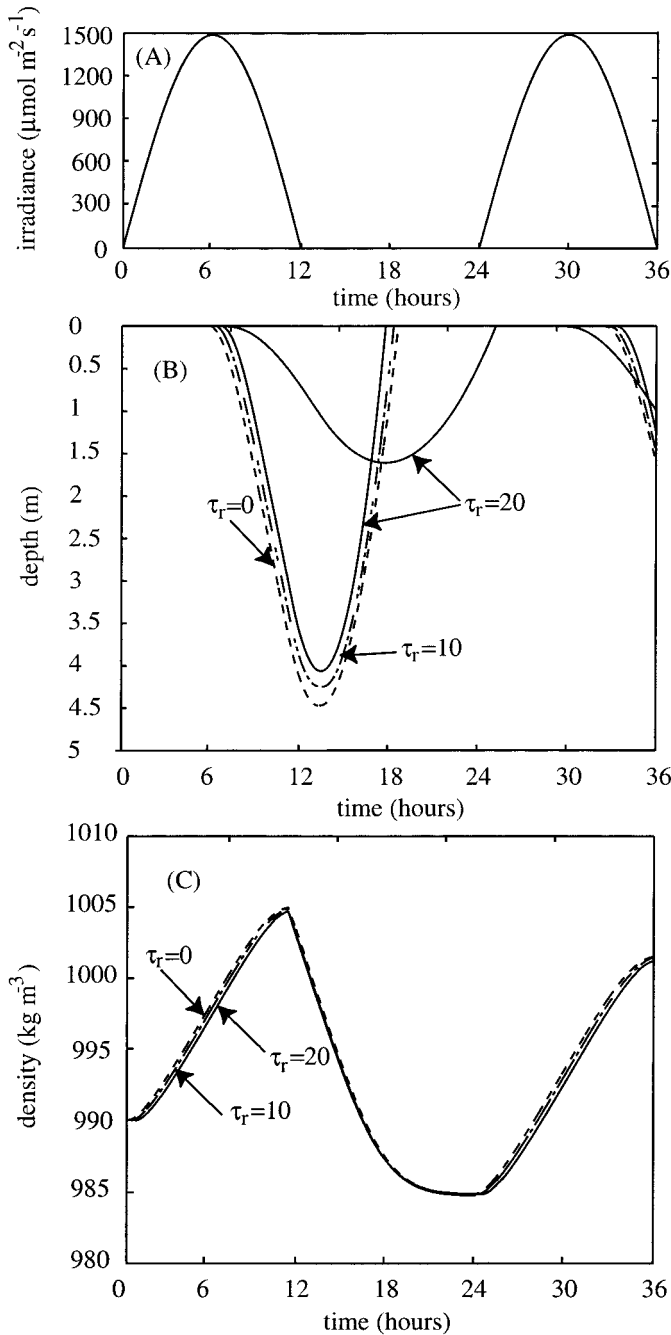


Fig. 4. Predicted diurnal vertical migration for *Microcystis aeruginosa* in a quiescent water column. (A) The light distribution for the simulation. (B) Simulation of colonies of diameter 800 μm and 200 μm . The larger colony sinks to a greater depth than does the smaller one. The 800- μm colony is plotted for no response time and response times of $\tau_r = 10$ and 20 min, and the 200- μm colony is plotted for $\tau_r = 20$ min only. The initial density for all colonies is 990 kg m^{-3} . (C) The corresponding change in cell density for the simulations in (B) for the 800- μm colonies. The density changes for the 200- μm colony are not plotted but are of identical form to those for the 800- μm colonies.

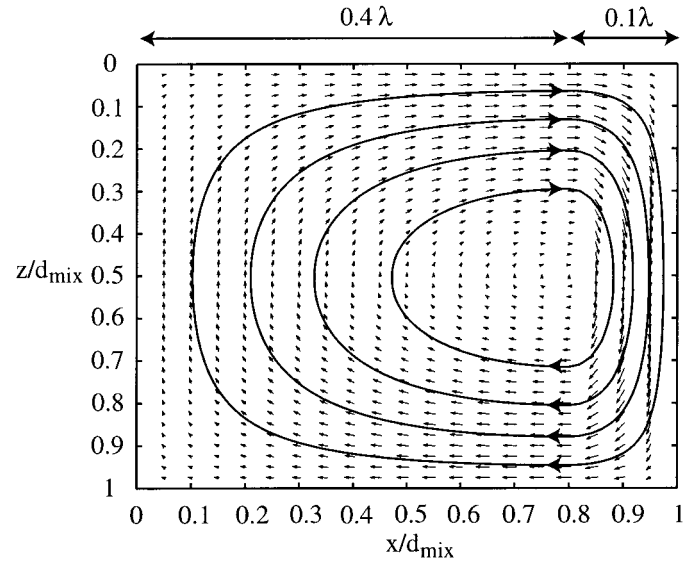


Fig. 5. Velocity field and associated streamlines following the Buranathanitt et al. (1982) Langmuir cell model. The width (x) and depth (z) are nondimensionalized by the mixed-layer depth d_{mix} . A Langmuir circulation is comprised of adjacent cells circulating in alternating directions. Only one cell rotating clockwise is shown.

Case 2—In case 2, the model of buoyancy regulation was coupled to a simple model of Langmuir circulation. Although the existence of Langmuir cells in the upper layer of lakes has been recognized for many years, the mechanisms of Langmuir cell circulation are still not well understood. We assumed the model of Langmuir cell circulation proposed by Buranathanitt et al. (1982).

The Buranathanitt et al. (1982) model assumes that the downwelling velocity is significantly larger than the upwelling velocity and is contained in a region that is a factor of 0.1 of the horizontal wavelength of the Langmuir cell (Fig. 5). The motion is assumed to be fully laminar. The model equations are

$$u = \begin{cases} u^* \sin\left(\frac{5\pi x}{4\lambda}\right) \cos(\pi z), & 0 \leq x \leq 0.4\lambda \\ u^* \sin\left(\frac{5\pi}{2} - \frac{5\pi x}{\lambda}\right) \cos(\pi z), & 0.4\lambda \leq x \leq 0.5\lambda \end{cases}$$

$$w = \begin{cases} -\frac{5}{4\lambda} u^* \cos\left(\frac{5\pi x}{4\lambda}\right) \sin(\pi z), & 0 \leq x \leq 0.4\lambda \\ \frac{5}{\lambda} u^* \cos\left(\frac{5\pi}{2} - \frac{5\pi x}{\lambda}\right) \sin(\pi z), & 0.4\lambda \leq x \leq 0.5\lambda \end{cases} \quad (13)$$

where u and w are the horizontal and vertical velocities respectively, λ is the nondimensional horizontal cell wavelength, and x and z are the horizontal and vertical coordinates, respectively. The depth of the Langmuir circulation is equivalent to the depth of the mixed layer d_{mix} , so that $\lambda = 2 d_{\text{mix}}$. The speed of rotation is governed by the wind speed U_w through the parameter $u^* = C_D U_w$, where $C_D = 0.85 \times$

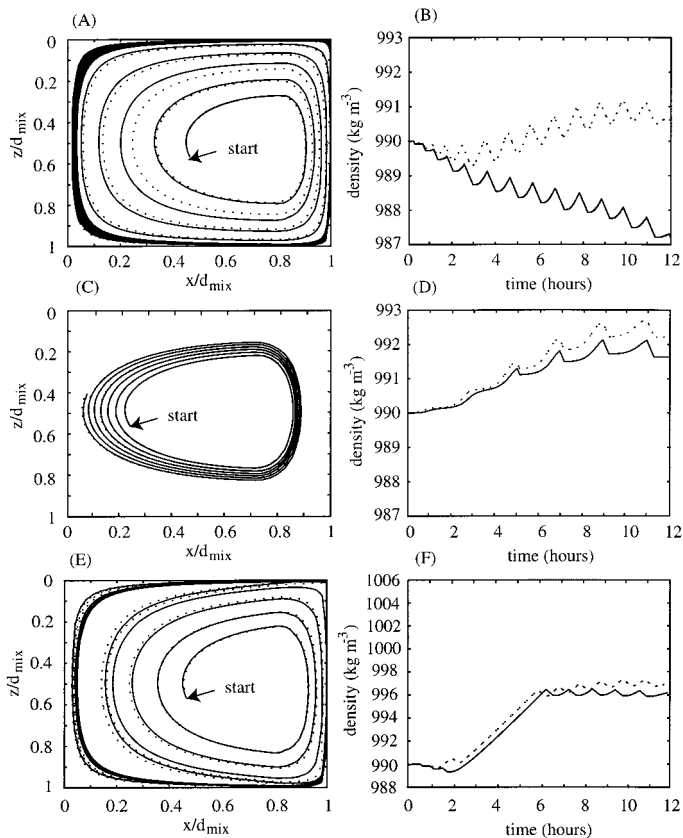


Fig. 6. Colony trajectories and the corresponding density fluctuations in a Langmuir cell. The solid line is for a colony with $\tau_r = 20$ min, and the dotted line is for a colony with no response time. (A) Trajectory for a 200- μm colony and $U_w = 5 \text{ m s}^{-1}$, with the corresponding density variation (B). (C) Trajectory for a 200- μm colony and $U_w = 1 \text{ m s}^{-1}$, with the corresponding density variation (D). (E) Trajectory for an 800- μm colony with $U_w = 5 \text{ m s}^{-1}$, with the corresponding density variation (F).

10^{-2} is the drag coefficient. Figure 5 shows the velocity field generated by the model equations and the streamlines of four neutrally buoyant particles.

The coupled simulation involved placing a colony in the flow field shown in Fig. 5 and tracking its position. At each time step, the density of the colony is calculated and its sinking or rising velocity is determined using Stokes's equation. This velocity is then added vectorially to the flow velocity vector corresponding to the position of the colony within the flow field. The position of the colony is then updated and the process repeated until the end of the simulation. In all simulations, the time step was set to 0.1 s. This small value was chosen so that the numerical integration of Eq. 5 was extremely accurate (truncation error \approx (time step)³).

The results of three simulations with different values of wind speed and colony size are shown in Fig. 6. All three simulations had two colonies initially at a density of 990 kg m^{-3} , one with a long response time ($\tau_r = 20$ min) and the other with no response time (i.e., $K_r = 0$ or $D = D_{eq}$). All simulations were run over one photoperiod (i.e., 12 h), although the simulations could easily have been run for much

longer (the figures would become too cluttered and no extra information is provided from longer simulations).

In the first simulation ($U_w = 5 \text{ ms}^{-1}$, colony size = 200 μm), the colonies migrate rapidly to the perimeter of the cell where they circulate until the end of the simulation (Fig. 6A,B). This circulation pattern causes the colonies to experience surface light intensity and complete darkness in each circulation and results in a continual cycle of density increase in the light and density decrease in the dark. In Fig. 6B, the colony with $\tau_r = 20$ min undergoes a reduction in density over one photoperiod as compared with the density increase shown in Fig. 4C for the no-water-motion case. The colony with no response time increases its density over the photoperiod and so reduces its buoyancy.

In the second simulation of case 2 ($U_w = 1 \text{ ms}^{-1}$, colony size = 200 μm), the rate of circulation is slower and the colonies remain in the interior of the Langmuir cell, where they experience smaller light fluctuations than in the previous simulation. The effect of the response time on the density fluctuations is reduced.

In the third simulation of case 2 ($U_w = 5 \text{ ms}^{-1}$, colony size = 800 μm), the effect of a larger colony can be contrasted with the results shown in Fig. 6A. The colonies migrate rapidly to the exterior of the Langmuir cell, but this time the colonies remain on the surface during the 2–6 h interval (Fig. 7). During this time, the density of the colonies increases rapidly and buoyancy is reduced to the point where the colonies are entrained back into the Langmuir circulation. Once the colonies have been re-entrained, the rate of change in density is greatly reduced.

Case 3—The final simulations (case 3) involved investigating the effect on the buoyancy regulation model of complex disorganized motion associated with turbulence. Turbulent velocity scales in the mixed layer of lakes are characterized, for wind-induced motions, by a complex velocity field, the exact quantitative nature of which is unknown. However, to illustrate the effect of turbulence on the buoyancy regulating mechanism of cyanobacteria we assumed an idealized case of isotropic and stationary turbulence represented by a random walk model.

Two typical simulations of the turbulence scenario are shown in Fig. 8. Only two results are shown; however, all other simulations produce similar results. The density variation in the presence of turbulent motion is small. The effect of the response time is to restrict changes in the buoyancy state of the colony because the colony is in a constant state of adjustment, and if the time scale of the light fluctuations is smaller than the response time, then the colony's rate of density change will never reach a state of equilibrium.

Discussion

Buoyancy-regulating cyanobacteria are exposed to a complex velocity field resulting from wind stirring, surface heating and cooling, and shear production in lakes (Patterson et al. 1994). The path along which gas-vacuolate cyanobacterial cells or colonies are transported in a water body depends on the motions of the currents, eddies, and waves and on the state of buoyancy of the cells or colonies. Thus, cya-

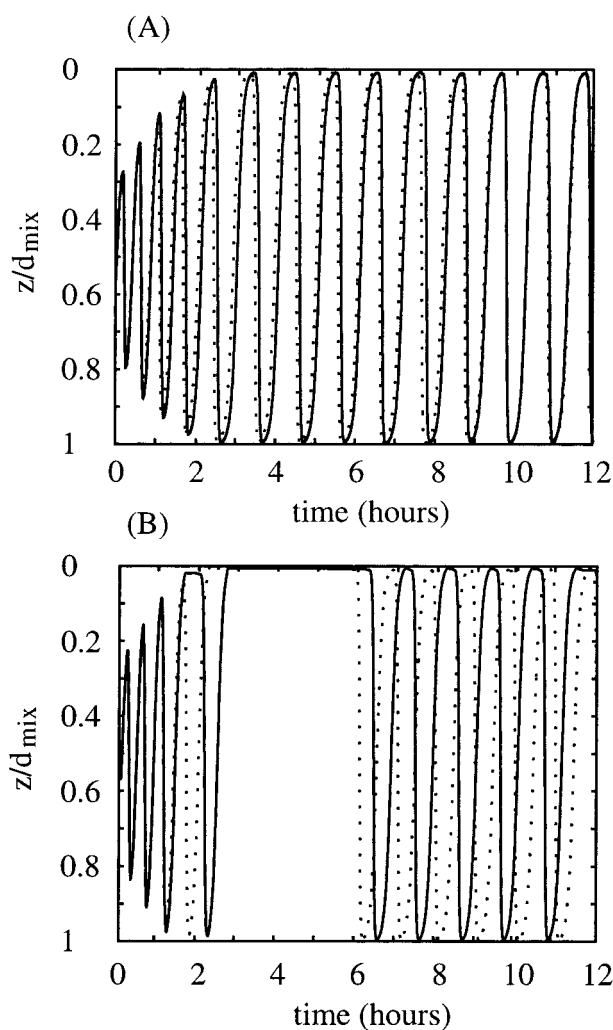


Fig. 7. Colony depth histories in a Langmuir cell. The solid line is for a colony with $\tau_r = 20$ min, and the dotted line is for a colony with no response time. (A) Depth history for a 200- μm colony and $U_w = 5$ m s $^{-1}$. (B) Depth history for a 800- μm colony and $U_w = 5$ m s $^{-1}$. These figures correspond to the plots of trajectories and density variations shown in Fig. 6A, 6B, 6E, and 6F, respectively.

nobacteria in a mixed layer follow a path determined by both the water velocity field and the rising or falling motions determined by its buoyancy.

The turbulent velocity scales characterize the light fluctuations to which cyanobacterial cells or colonies are exposed during mixing. For wind induced motions, the turbulent velocity scale, u^* , typically is three orders of magnitude lower than the wind speed ($u^* = U_w \times 10^{-3}$). Assuming that the turbulent eddy scale is of the order of the mixed layer depth, d_{mix} , then the fluctuation time scale is d_{mix}/u^* . Thus, for a 2 m s $^{-1}$ wind speed and 2-m mixed layer depth, this time scale is approximately 20 min. Thus, if the euphotic depth is shallower than the mixed-layer depth, cells entrained in turbulence may experience light fluctuations from darkness to surface-level irradiance on time scales of 20 min.

Our study is the first to examine the process of buoyancy

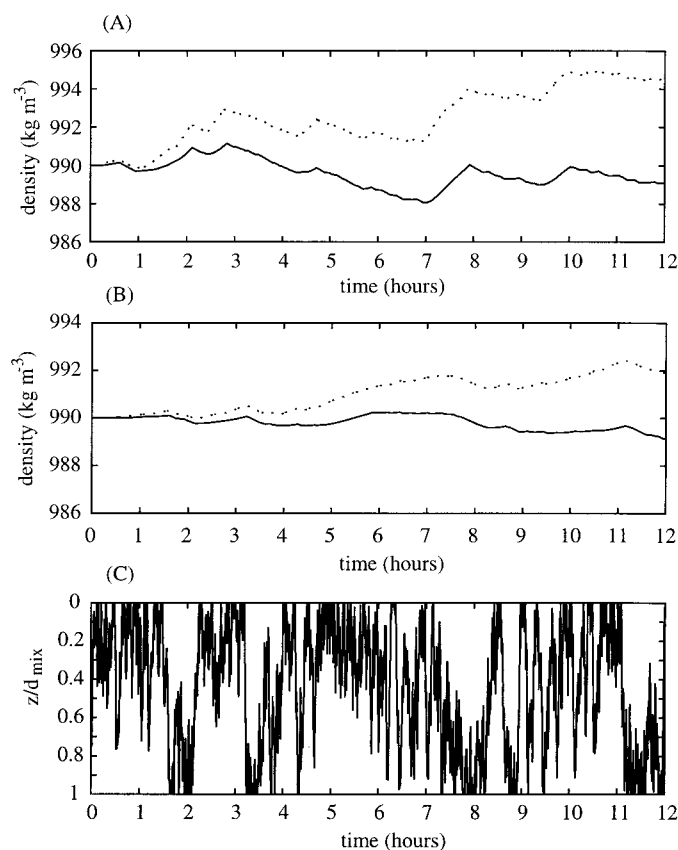


Fig. 8. (A) Density fluctuations for an 800- μm colony in a turbulent flow field with a response time $\tau_r = 20$ min (solid line) and no response time (dashed line). (B) Density fluctuations for a 200- μm colony. (C) Corresponding depth history for the density variation in (A).

regulation at the short time scales relevant to the light fluctuations experienced by cells during turbulent mixing. Measurements over short time intervals show that there is an initial nonlinear response period in the rate of carbohydrate accumulation after an increase in light. This finding contradicts previous assumptions that the rate of carbohydrate accumulation adjusts instantaneously to an increase in light. However, Kromkamp and Walsby (1990) used a measuring frequency of 1 h, and any initial nonlinear response may have occurred during the first hour. Visser et al. (1997) also noted an initial nonlinear response period and found that the rate of increase of carbohydrate content in *Microcystis* reached steady-state 15–20 min after an increase in irradiance. The nonlinear response is of critical importance because when the time scale of the light fluctuations is similar to that of the nonlinear response the density change may be continually nonlinear. Thus, a model that will be used to predict the buoyancy of cyanobacteria in frequently mixed water bodies must include this nonlinear response.

The ability of our model to reproduce the experimental data is taken as a strong argument for incorporating a nonlinear response of this form. Our model is, however, empirical and makes no attempt to account for the physiological or biochemical processes that interact to cause the observed

density change response. Carbohydrate ballast is produced by the assimilation of CO₂ via the reductive pentose-phosphate cycle during photosynthesis. The properties of the assimilation cycle determine the conditions under which storage of carbohydrate (as polyglucose) occurs. When a cell is actively growing, intermediates will be removed from the assimilation cycle at various points for the synthesis of cell constituents in a balanced manner (Ihlenfeldt and Gibson 1975). If the rate of CO₂ assimilation is greater than the requirements for intermediates, the excess will be stored as polyglucose. If cell growth is suspended (perhaps because of limiting nutrients), intermediates are no longer removed and all CO₂ assimilated is stored as polyglucose (Pelroy et al. 1972). Factors such as light intensity, CO₂, and nutrient availability are important in determining the rate of polyglucose accumulation but are not important in determining the time required for adaptation to an increase in the irradiance. Instead, the nonlinear response may be the result of a period of adaptation of the photosynthetic apparatus or adaptation of the reductive pentose-phosphate cycle to a change in the rate of supply of carbon, or a combination of both. However, the processes that govern the relationship between photosynthetic activity and the rate of carbohydrate accumulation are complex and beyond the scope of this study.

Harris and Piccinin (1977) investigated the photosynthetic behavior of natural populations of phytoplankton and found that when suddenly exposed to a change in light intensity, the photosynthetic rate took between 15 and 60 min to reach a steady state. The existence of a response time for buoyancy change could thus be expected from the existence of photosynthetic response times. Our model for buoyant density change is based on the same equations used by Pahl-Wostl and Imboden (1990) to model the relationship between fluctuating light and photosynthetic response times. Because the short-term ballast changes are caused by changes in polyglucose produced through photosynthesis, it is not surprising that the equations that describe the dynamic photosynthetic responses can be used to describe the dynamic buoyancy regulation responses.

The main departure of our model from previous models is that the rate of change in cell density versus irradiance is not determined by a single curve but by a family of curves. These curves represent an adjustment in the rate of density change until, after a period corresponding to the response time, all subsequent curves coalesce to a single curve (the equilibrium or steady-state curve, D_{eq}). It is also evident from Fig. 2E that if the light is fluctuating on time scales less than the response time, then the rate of density change will never reach equilibrium. It will be at some nonequilibrium value determined by the light history, the light variation, and the response time.

Validation of our model with the measurements of Visser et al. (1997) revealed that incorporation of the response time could explain the small discrepancy between their measured and predicted values. Different response times were observed between the present study ($\tau_r = 20$ min) and that of Visser et al. ($\tau_r = 4$ min). Our *Microcystis* strain was extracted directly from the field, where it was commonly exposed to surface level irradiances, and there was no inhibition in the rate of carbohydrate accumulation at high

irradiance levels. By contrast, the *Microcystis* strain used in experiments by Visser et al. (1997) was cultured in the laboratory at low irradiances and showed strong inhibition in the rate of carbohydrate ballast accumulation above 400 $\mu\text{mol photons m}^{-2} \text{ s}^{-1}$.

The density of the cells or colonies after mixing depends critically on the response time. In all our simulations, the colonies with the 20-min response time did not accumulate as much carbohydrate ballast as did the colonies with no response time. The colonies with the 20-min response time needed time to adjust the rate of carbohydrate accumulation to increases in irradiance. The colonies with no response time could instantaneously increase the rate of carbohydrate ballast accumulation in response to increases in irradiance. However, our results also indicate that there are conditions under which the effect of the response time is reduced. If the time scale of the light fluctuations is long compared with the response time, then the rate of carbohydrate accumulation can equilibrate and the effect of the response time will be small (see Fig. 6C,D). Also, colonies may be unaffected by the mixing if their inertial force is larger than the entraining force of the mixing (see Fig. 7). Under these conditions, the effect of the response time will be small (as in the no-mixing case), and carbohydrate will be accumulated at the equilibrium rate.

When wind stirring causes the *Microcystis* colonies to be entrained from the surface, a long response time may allow maintenance of positive buoyancy during turbulence and a rapid return to the surface when the turbulence subsides. Thus, the response time may be an ecological adaptation of some species to the light climate resulting from entrainment in fluid motion. A long response time might represent an adaptation of a species that spends significant time at the water surface. For example, *Microcystis* are commonly adapted to high surface irradiances (Zohary and Robarts 1989). A long response time delays the onset of sinking away from the surface under calm conditions, resulting in the colonies receiving a higher light dose in the morning (Fig. 4), making shallower migrations and returning to the surface earlier than those with shorter response times. Long response times may also be more common in colony-forming species. These species would spend more time at the surface because they are able to sink and float at greater speeds and so quickly return to the surface after a mixing event. They are also commonly able to overcome the entraining forces of the water motion (see Fig. 6E,F) to remain at the water surface when positively buoyant. Conversely, a short response time might represent an adaptation of a species that is frequently exposed to a fluctuating light climate experienced when entrained into the turbulent motions. Such a species might form small colonies or no colonies. In this case, the response time must be fast relative to the time scale of the light fluctuation if the cells or colonies are to be able to adjust their buoyancy.

An understanding of the processes that determine the spatial and temporal distribution of cyanobacteria in lakes and reservoirs is central to the control and management of problem blooms of these species. One process that is important to the ecology of certain cyanobacteria is their ability to migrate vertically through the water column. An understand-

ing of the mechanisms that control vertical migration in cyanobacteria has developed rapidly, and our work provides the basis upon which a detailed understanding of the effect of water motion on vertical migration can be established.

References

- ALLISON, E. M., AND A. E. WALSBY. 1981. The role of potassium in the control of turgor pressure in a gas-vacuolate blue-green alga. *J. Exp. Bot.* **32**: 241–249.
- BURANATHANITT, T., D. J. COCKRELL, AND P. H. JOHN. 1982. Some effects of Langmuir circulation on the quality of water resource systems. *Ecol. Modell.* **15**: 49–74.
- DEACON, C., AND A. E. WALSBY. 1990. Gas vesicle formation in the dark, and in the light of different irradiances, by the cyanobacterium *Microcystis* sp. *Br. Phycol. J.* **25**: 133–139.
- GANF, G. G., AND R. L. OLIVER. 1982. Vertical separation of light and available nutrients as a factor causing replacement of green algae by blue-green algae in the plankton of a stratified lake. *J. Ecol.* **70**: 829–844.
- GRANT, N. G., AND A. E. WALSBY. 1977. The contribution of photosynthate to turgor pressure rise in the planktonic blue green alga *Anabaena flos-aquae*. *J. Exp. Bot.* **28**: 409–415.
- HARRIS, G. P., AND B. B. PICCININ. 1977. Photosynthesis by natural phytoplankton populations. *Arch. Hydrobiol.* **80**: 405–456.
- HEBBERT, D. P. J., P. J. PHIPPS, AND R. W. STRANGE. 1971. Chemical analysis of microbial cells, p. 209–344. *In* J. R. Norris and D. W. Ribbons [eds.], *Methods in microbiology*. V. 5B. Academic Press.
- HOWARD, A., A. E. IRISH, AND C. S. REYNOLDS. 1996. A new simulation of cyanobacterial underwater movement (SCUM'96). *J. Plankton Res.* **18**: 1375–1385.
- HUMPHRIES, S. E., AND V. D. LYNE. 1988. Cyanophyte blooms: The role of cell buoyancy. *Limnol. Oceanogr.* **33**: 79–91.
- IBELINGS, B. W., L. R. MUR, AND A. E. WALSBY. 1991. Diurnal changes in buoyancy and vertical distributions in populations of *Microcystis* in two shallow lakes. *J. Plankton Res.* **13**: 419–436.
- IHLENFELDT, M. J. A., AND J. GIBSON. 1975. CO₂ fixation and its regulation in *Anacystis nidulans* (*Synechococcus*). *Arch. Microbiol.* **102**: 13–21.
- KLEMER, A. R. 1978. Nitrogen limitation of growth and gas vacuolation in *Oscillatoria rubescens*. *Verh. Int. Ver. Limnol.* **20**: 2293–2297.
- . 1991. Effects of nutritional status on cyanobacterial buoyancy, blooms, and dominance, with special reference to inorganic carbon. *Can. J. Bot.* **69**: 1133–1138.
- KONOPKA, A. E., A. R. KLEMER, A. E. WALSBY, AND B. W. IBELINGS. 1993. Effects of macronutrients upon buoyancy regulation by metalimnetic *Oscillatoria agardhii* in Deming Lake, Minnesota. *J. Plankton Res.* **15**: 1019–1034.
- KROMKAMP, J., A. KONOPKA, AND L. R. MUR. 1986. Buoyancy regulation in a strain of *Aphan* (Cyanophyceae): The importance of carbohydrate accumulation and gas vesicle collapse. *J. Gen. Microbiol.* **132**: 2113–2121.
- , ———, AND ———. 1988. Buoyancy regulation in light limited continuous cultures of *Microcystis aeruginosa*. *J. Plankton Res.* **10**: 171–183.
- , AND L. R. MUR. 1984. Buoyant density changes in the cyanobacterium *Microcystis aeruginosa* due to changes in the cellular carbohydrate content. *FEMS Microbiol. Lett.* **25**: 105–109.
- , AND A. E. WALSBY. 1990. A computer model of buoyancy and vertical migration in cyanobacteria. *J. Plankton Res.* **12**: 161–183.
- LANGMUIR, I. 1938. Surface motion of water induced by winds. *Science* **87**: 119–123.
- MARRA, J. 1978. Effects of short term variations in light intensity on photosynthesis of a marine phytoplankter: A laboratory simulation study. *Mar. Biol.* **46**: 191–202.
- OLIVER, R. L., A. J. KINNEAR, AND G. G. GANF. 1981. Measurements of cell density of three freshwater phytoplankters by density gradient centrifugation. *Limnol. Oceanogr.* **26**: 285–294.
- , R. H. THOMAS, C. S. REYNOLDS, AND A. E. WALSBY. 1985. The sedimentation of buoyant *Microcystis* colonies caused by precipitation with an iron-containing colloid. *Proc. R. Soc. Lond. Ser. B* **223**: 511–528.
- , AND A. E. WALSBY. 1984. Direct evidence for the role of light-mediated gas vesicle collapse in the buoyancy regulation of *Anabaena flos-aquae* (cyanobacteria). *Limnol. Oceanogr.* **29**: 879–886.
- PAHL-WOSTL, C., AND D. M. IMBODEN. 1990. DYPHORA—a dynamic model for the rate of photosynthesis of algae. *J. Plankton Res.* **12**: 1207–1221.
- PATTERSON, J. C., D. P. HAMILTON, AND J. M. FERRIS. 1994. Modelling of cyanobacterial blooms in the mixed layer of lakes and reservoirs. *Aust. J. Mar. Freshwater Res.* **45**: 829–845.
- PELROY, R. A., R. RIPPKA, AND R. Y. STAINER. 1972. The metabolism of glucose by unicellular blue-green algae. *Arch. Microbiol.* **87**: 303–322.
- REYNOLDS, C. S. 1984. *The ecology of freshwater phytoplankton*. Cambridge Univ. Press.
- . 1987. Cyanobacterial water blooms. *Adv. Bot. Res.* **13**: 67–143.
- , R. L. OLIVER, AND A. E. WALSBY. 1987. Cyanobacterial dominance: The role of buoyancy regulation in the billowing environment. *N.Z. J. Mar. Freshwater Res.* **21**: 379–390.
- , AND A. E. WALSBY. 1975. Water blooms. *Biol. Rev.* **50**: 437–481.
- THOMAS, R. H., AND A. E. WALSBY. 1986. Buoyancy regulation in a strain of *Microcystis*. *J. Gen. Microbiol.* **131**: 799–809.
- UTKILEN, H. C., R. L. OLIVER, AND A. E. WALSBY. 1985. Buoyancy regulation in a red *Oscillatoria* unable to collapse gas vacuoles by turgor pressure. *Arch. Hydrobiol.* **102**: 319–329.
- VISSER, P. M., J. PASSARGE, AND L. R. MUR. 1997. Modelling vertical migration of the cyanobacterium *Microcystis*. *Hydrobiologia* **349**: 99–109.
- WALSBY, A. E. 1969a. The permeability of blue-green algal gas vacuole membranes to gas. *Proc. R. Soc. Lond. Ser. B* **173**: 235–255.
- . 1969b. Structure and function of gas vesicles. *Bacteriol. Rev.* **36**: 1–32.
- . 1970. The nuisance algae: Curiosities in the biology of planktonic blue-green algae. *Water Treat. Exam.* **19**: 359–373.
- . 1971. The pressure relationships of gas vacuoles. *Proc. R. Soc. Lond. Ser. B* **178**: 301–326.
- . 1994. Gas vesicles. *Microbiol. Rev.* **58**: 94–144.
- , R. KINSMAN, B. W. IBELINGS, AND C. S. REYNOLDS. 1991. Highly buoyant colonies of the cyanobacterium *Anabaena lemmermannii* form persistent surface waterblooms. *Arch. Hydrobiol.* **121**: 261–280.
- , H. C. UTKILEN, AND I. J. JOHNSEN. 1983. Buoyancy changes in a red coloured *Oscillatoria agardhii* in Lake Gjersjøen, Norway. *Arch. Hydrobiol.* **97**: 18–38.
- ZOHARY, T., AND R. D. ROBARTS. 1989. Diurnal mixed layers and the long-term dominance of *Microcystis aeruginosa*. *J. Plankton Res.* **11**: 25–48.

Received: 23 January 1998

Accepted: 24 September 1998

Amended: 22 October 1998